Supplementary Information

Defective/Graphitic-Synergy in Heteroatom-interlinked-triggered Metal-free Electrocatalyst for High-performance Rechargeable Zinc-Air Batteries

Ghulam Yasin [a, b], Sehrish Ibrahim [c], Shumaila Ibraheem [a, b] *, Sajjad Ali [d] *, Rashid Iqbal [a, b], Anuj Kumar [e] *, Mohammad Tabish [f], Yassine Slimani [g], Tuan Anh Nguyen [h], Hu Xu [d] *, Wei Zhao [a] *

[a] Institute for Advanced Study, Shenzhen University, Shenzhen 518060, Guangdong, China

[b] College of Physics and Optoelectronic Engineering, Shenzhen University, Shenzhen 518060, Guangdong, China

[c] College of Life Science and Technology, Beijing University of Chemical Technology, Beijing 100029, China

[d] Department of Physics, Southern University of Science and Technology, Shenzhen 518055, China

[e] Nano-Technology Research Laboratory, Department of Chemistry, GLA University, Mathura, Uttar Pradesh 281406, India

[f] State Key Laboratory of Chemical Resource Engineering, Beijing University of Chemical Technology, Beijing 100029, China

[g] Department of Biophysics, Institute for Research & Medical Consultations (IRMC), Imam Abdulrahman Bin Faisal University, Dammam 31441, Saudi Arabia

[h] Institute for Tropical Technology, Vietnam Academy of Science and Technology, VAST, Hanoi, Viet Nam

Corresponding Authors:

shumaila.ibraheem@yahoo.com (S. Ibraheem)
sajjad@alum.imr.ac.cn (S. Ali)
anuj.kumar@gla.ac.in (A. Kumar)
xuh@sustech.edu.cn (H. Xu)
weizzhao@szu.edu.cn (W. Zhao)

1. Experimental Section

The heteroatom-interlinked-triggered asphaltene material (D/G-HASP) was extracted from the asphalt via a facile fractionation approach named as SARA (saturates-aromatics-resins-asphaltenes), reported by R. Kessler and P. Cesti [1, 2]. In brief, hot toluene was faintly stirred for about 2 h with an asphalt powder (with volume to mass (V/m) ratio of 5:1) at the temperature of around 60 °C. Afterward, to isolate the filtrate and other residual as undissolved components, the solution was filtered using a membrane filter of 0.45-micron size. Later, toluene was isolated via using a rotary evaporator and the attained toluene-free product (asphalt) was then further treated with the solvent of n-heptane under of 40:1 V/m ratio for the successful precipitation of asphaltene. Subsequently, to prepare the non-filterable final product (D/G-HASP), the precipitated mixture was further sieved via using the membrane filter with size of 0.45 micron. To fully eliminate the present residues of waxy compounds, the sieved D/G-HASP was then finally cleaned with boiling solvent of n-heptane in a typical Soxhlet apparatus for about 35 h up until fully colorless filtrate solution achieved. Lastly, the attained dark-brown solid product (D/G-HASP) was further dried at 190 °C in a vacuum oven for over 20 h to evaporate the any remaining solvent. For comparison, N-doped carbon (N-C) and S-doped carbon (S-C) catalysts were prepared by simply heating the mixture of sucrose and melamine, and mixture of thiophene and sucrose, respectively at 850 °C for 2 h under Ar atmosphere. Similarly, graphene or graphitic carbon (GC) and annealed graphene or defective carbon (D-C) were also prepared, graphene (GC) was prepared according to our previous work [3],

and annealed graphene (DC) was synthesized simply by heating the GO in air at 400 °C for 3 h, with a ramping rate of 10 °C min^{-1}. Throughout this annealing process, the gas inlet of the tube furnace was closed and the outlet stayed open.

2. Material Characterization

The Morphology of as acquired electrocatalysts was characterized by FESEM, TEM and HRTEM. The FESEM images were taken on a JSM-7800F (JEOL) scanning electron microscope recorded at an acceleration voltage of 8.0 kV. The TEM and HRTEM images were also obtained from JEM-2100F, with using a standard operating voltage of 200 kV. The elemental composition was determined by scanning electron microscopy (Hitachi S-4700) and its attached EDAX micro analyzer. The crystal structure was characterized by XRD. The XRD data of the as-prepared material were achieved using an X-ray diffractometer (D2 PHASER from Bruker Company, Germany) with using Cu Kα radiation (λ = 1.540 56 Å). Further validation of produced material was performed by Fourier transform infrared (FTIR) spectroscopic evaluation that was directed through KBr pellets with a FTIR spectrometer (Nicolet 6700 FT-IR from Thermo Scientific, USA). Raman spectra were also achieved from the Horiba LabRAM HR Evolution employing a laser of excitation wavelength of 532 nm at room temperature. The X-ray photoelectron spectrometry (XPS) examination was performed on Thermo VG ESCALAB MK II with employing Al Kα radiation. Similarly, nitrogen adsorption/desorption isotherms were accomplished via an ASAP 2460 N_2 adsorption apparatus for the Porosity Analyzer and Surface Area (Micrometritica, USA).

3. Electrochemical Measurements

All the electrochemical tests for both ORR and OER procedures were evaluated by the autolab electrochemical workstation. The electrochemical examination towards ORR and OER were tested by three-electrode method in which reference electrode (vs Ag/AgCl), graphite rod as counter electrode and working electrode (glassy carbon rotating disk) were used in alkaline medium (0.1 M KOH electrolyte) under O_2-/N_2-infested. In this work all the potentials are set relative to a reversible hydrogen electrode (RHE). For working electrode, uniform catalyst ink was prepared by ultra-sonicating 2 mg of sample in 800 µL ethanol and 15 µL of Nafion (5% solution) for 30 minutes. Then, catalyst ink was spread on a glassy carbon surface (0.19625 cm^2) followed by drying before functioning the tests. The catalysts loading were ~0.25 mg cm^{-2}. Commercial IrO_2 and 20 wt% Pt/C catalysts were used as the standard catalysts. And working-electrodes were prepared by 0.25 mg cm^{-2} and 40µg cm^{-2} mass loading for the commercial IrO_2 and 20 wt% Pt/C catalyst respectively. The Linear Sweep Voltammetry curves were checked in 0.1 M KOH electrolyte at 10 mVs^{-1} of voltage sweeping-rate, respectively for both ORR and OER. For ORR stability the accelerated durability test (ADT) was performed in oxygen flooded 0.1 M KOH electrolyte at room temperature by applying potential sweeps between 0.6&1.2 V at sweeping rate of 50 mVs^{-1} for 10000 CV cycles. To analyze the electron transfer numbers (n) with Koutecky-Levich equations, the ORR LSV curves were performed at different rotations from 100 to 2500 rpm at 10 mV s^{-1} scan rate.

$$\frac{1}{j} = \frac{1}{j_L} + \frac{1}{j_K} = \frac{1}{Bw^{\frac{1}{2}}} + \frac{1}{j_K}$$

$$B = 0.62nFC_0(D_0)^{2/3}v^{-1/6}$$

$$j_K = nFkC_0$$

where $j_L$and j_K are the diffusion and kinetic-limiting current densities, j is the

measured current density, respectively; ω is the angular velocity of the disk; F is the Faraday constant (F = 96485 C mol^{-1}); n represents the overall number of electrons transferred during oxygen reduction; D_0 is the diffusion coefficient of O_2 in 0.1 M KOH solution; C_0 is the bulk concentration of O_2; v is the kinematics viscosity for electrolyte, and k is the electron-transferred rate constant. Electrochemical impedance spectroscopy (EIS) analysis were tested in O_2-saturated 0.1 M KOH electrolyte for ORR at 0.80 V vs. RHE with 10 mV ac potential from 10 kHz to 0.01 Hz and for OER at 0.30 V vs. RHE with 10 mV ac potential from 10 kHz to 0.01 Hz. The electrode-rotation speed was set at 1600 rpm.

4. Zinc-Air Batteries Test

A home-made plastic cell was used to fabricate the zinc-air battery. The gas diffusion layer (GDL) was made firstly by diffusing polytetrafluoroethylene (PTFE) emulsion (60 wt%, Saibo electrochemical) on the carbon paper, and then heated it at 340°C for 2 hours in muffle furnace. The air-electrode was equipped by transporting an assured volume of catalyst ink onto the carbon paper substrate with 0.25 mg cm^{-2}catalyst loading. A polished zinc plate (0.3 mm thickness) was used as anode. 6.0 M KOH was used as electrolyte for both primary and rechargeable zinc-air batteries to promise the revocable zinc electrochemical reactions at the Zn anode. The GDL has an effective area of 1 cm^2 and lets O_2 to influence the catalyst sites. Ni foam was used as current collector. All the zinc-air batteries were evaluated under ambient environment. The polarization curve measurements were achieved by LSV (5 mV s^{-1}) at 30°C with Versa STAT 4 electrochemical working station. Both the power density and the corresponding current density were standardized to the operative surface area of air electrode. The energy density and specific capacity were calculated according the following equation:

$$Specific\ Capacity = \frac{current * service\ hours}{weight\ of\ consumed\ zinc}$$

LAND testing system was used to analyze the galvanostatic charging-discharging cycling performance (6 minute/cycle).

5. Computational Framework

5.1. Calculation details

Density functional theory (DFT) calculations have been carried out using generalized gradient approximation (GGA) in the form of Revised Perdew-Burke-Ernzerhof (RPBE)[4] for the exchange-correlation potentials, as implemented in the Vienna ab initio simulation package (VASP), with consideration of spin-polarization[5-7]. A 3×1×1 k-points mesh and 400 eV energy cutoffs have been used to optimize structures of asphaltene and 3×3×1 k-points mesh for graphene. To described van der Waals corrections to DFT calculations, we included DFT-D3 correction method of Grimme[8]. In optimizing atomic structures, the force convergence criterion was set to 0.05 eVÅ^{-1}. The D/G-HASP unit cell is hexagonal 12.3 × 24.6 × 12.3 Å^3 for x, y, and z-direction, and the periodic condition is employed along x direction. The energies of gas-phase molecules (H_2, H_2O, and O_2) were calculated in a box in the size of 27 Å × 27 Å × 20 Å. The distance between neighboring cells is ~18 Å, to avoid the interaction between periodic images.

In this work the oxygen reduction reaction (ORR) is carried-out using the following 4 e$^-$ scheme at alkaline conditions.

$$O_{2(g)} + 2H_2O_{(l)} + 4e^- + * \rightarrow OOH^* + H_2O_{(l)} + OH^- + 3e^- \quad \text{(S1)}$$

$$OOH^* + H_{2(l)} + OH^- + 3e^- \rightarrow O^* + H_2O_{(l)} + 2OH^- + 2e^- \quad \text{(S2)}$$

$$O^* + H_2O_{(l)} + 2OH^- + 2e^- \rightarrow OH^* + 3OH^- + e^- \quad \text{(S3)}$$

$$OH^* + 3OH^- + e^- \rightarrow * + 4OH^- \quad \text{(S4)}$$

The asterisk (*) denotes the active site on D/G-HASP, (l) and (g) refer to gas and liquid phases, respectively, and OOH^*, O^* and OH^* are adsorbed intermediates.

The Gibbs free energy of the species involved in ORR is defined as

$$G = E_{DFT} + E_{ZPE} - TS \qquad \text{(S5)}$$

Where E_{DFT}, E_{ZPE}, and TS denoted the electronic energy, zero-point energy, and entropy at room temperature (T=298.15 K) respectively. The ZPE and entropies of ORR intermediates were calculated based on the vibrational frequencies. The E_{ZPE} and entropy of gas-phase molecules and reaction intermediates are listed in Table S1. The computational hydrogen electrode (CHE) model was used to calculate the Gibbs free energy for the reaction step involving the coupled proton-electron, in which the free energy of a pair of proton and electron ($H^+ + e^-$) was calculated as a function of applied potential relative to a reversible hydrogen electrode (U *vs* RHE), i.e., $\mu(H^+) + \mu(e^-) = \frac{1}{2}\mu(H_2) - eU_{RHE}$[9]. the adsorption free energies of OOH^*, O^* and OH^* at a given potential U_{RHE} can be calculated relative to H_2O and H_2.

$$\Delta(O_2) = 4.92 - 4eU_{RHE} \qquad \text{(S6)}$$

$$\Delta(OOH^*) = G(OOH^*) + \frac{3G(H2)}{2} - G(*) - 2G(H_2O) - 3eU_{RHE} \qquad \text{(S7)}$$

$$\Delta(O^*) = G(O^*) + G(H_2) - G(*) - G(H_2O) - 2eU_{RHE} \qquad \text{(S8)}$$

$$\Delta(OH^*) = G(OH^*) + \frac{G(H2)}{2} - G(*) - G(H_2O) - eU_{RHE} \qquad \text{(S9)}$$

The Gibbs free energy change for steps (1)-(4) can be expressed as

$$\Delta G_1 = \Delta(OOH^*) - \Delta G(O_2) \qquad \text{(S10)}$$

$$\Delta G_2 = \Delta(O^*) - \Delta G\,(OOH^*) \qquad \text{(S11)}$$

$$\Delta G_3 = \Delta(OH^*) - \Delta G(O^*) \qquad \text{(S12)}$$

$$\Delta G_4 = -\Delta(OH^*) \qquad \text{(S13)}$$

Using this approach, the theoretical overpotential (η) of ORR is calculated as

$$\eta = \max\,[\Delta G_1, \Delta G_2, \Delta G_3, \Delta G_4]/e - 1.23 \qquad \text{(S14)}$$

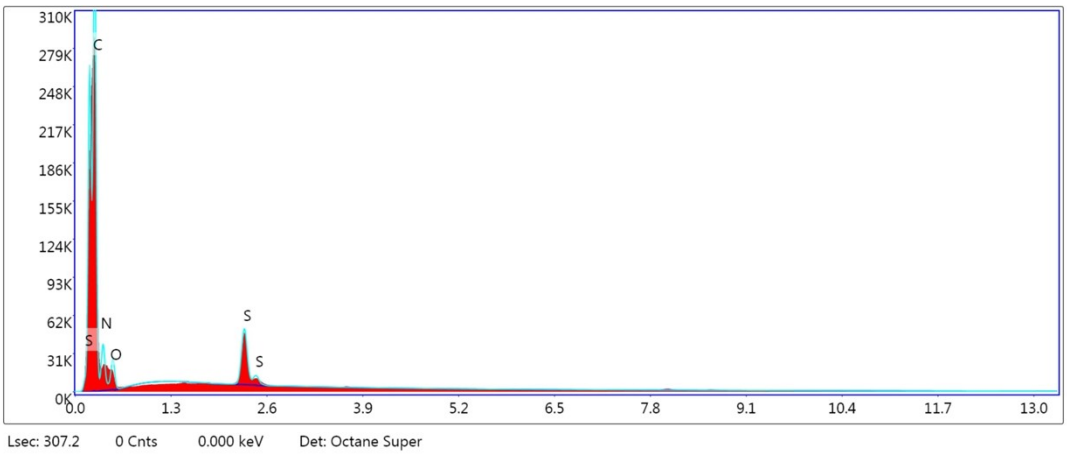

Fig. S1 EDS pattern of elemental composition of D/G-HASP material.

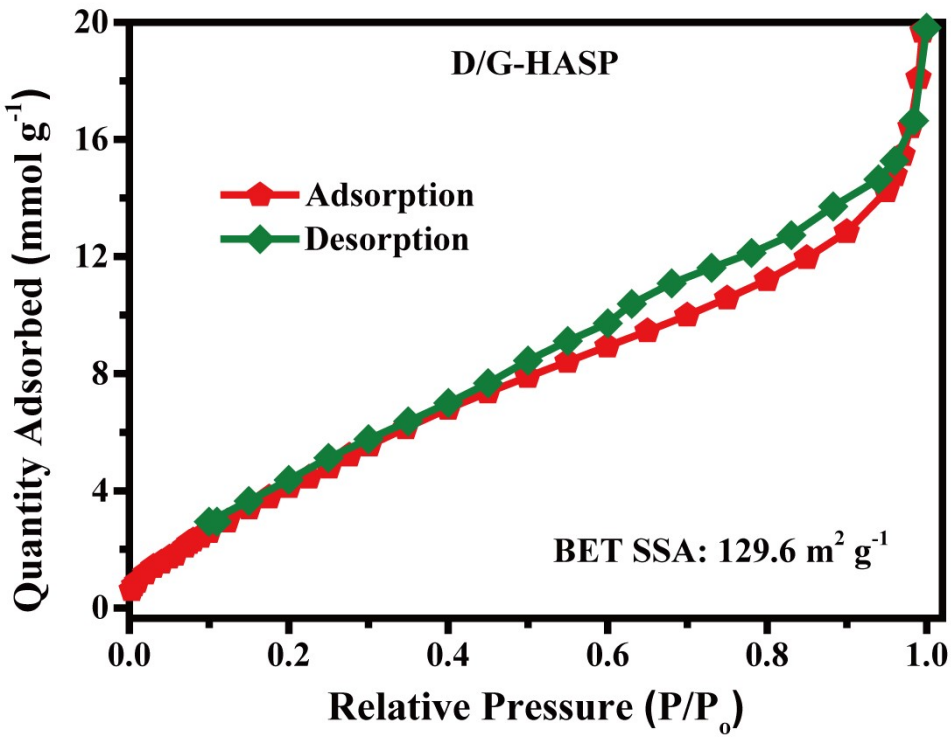

Fig. S2 Nitrogen adsorption-desorption isotherms of D/G-HASP catalyst.

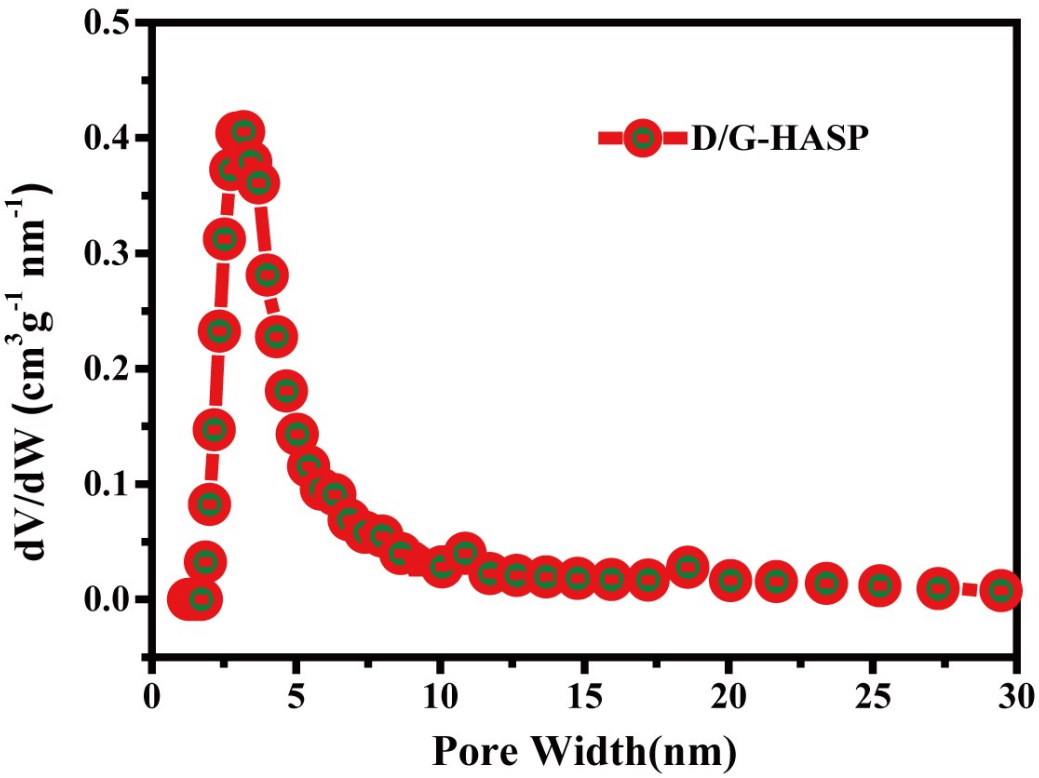

Fig. S3 Pore size distribution of D/G-HASP catalyst.

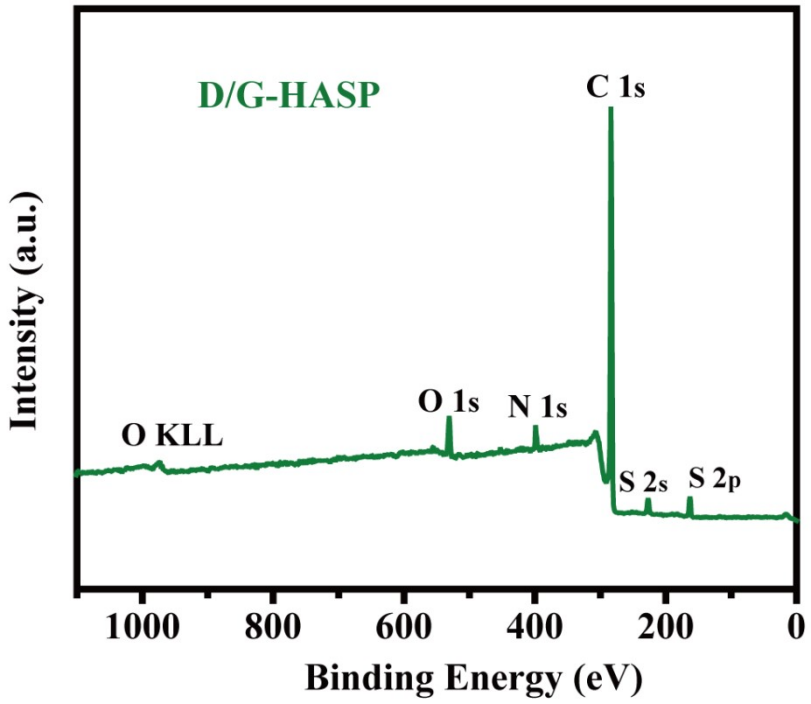

Fig. S4 XPS survey spectra of D/G-HASP catalyst.

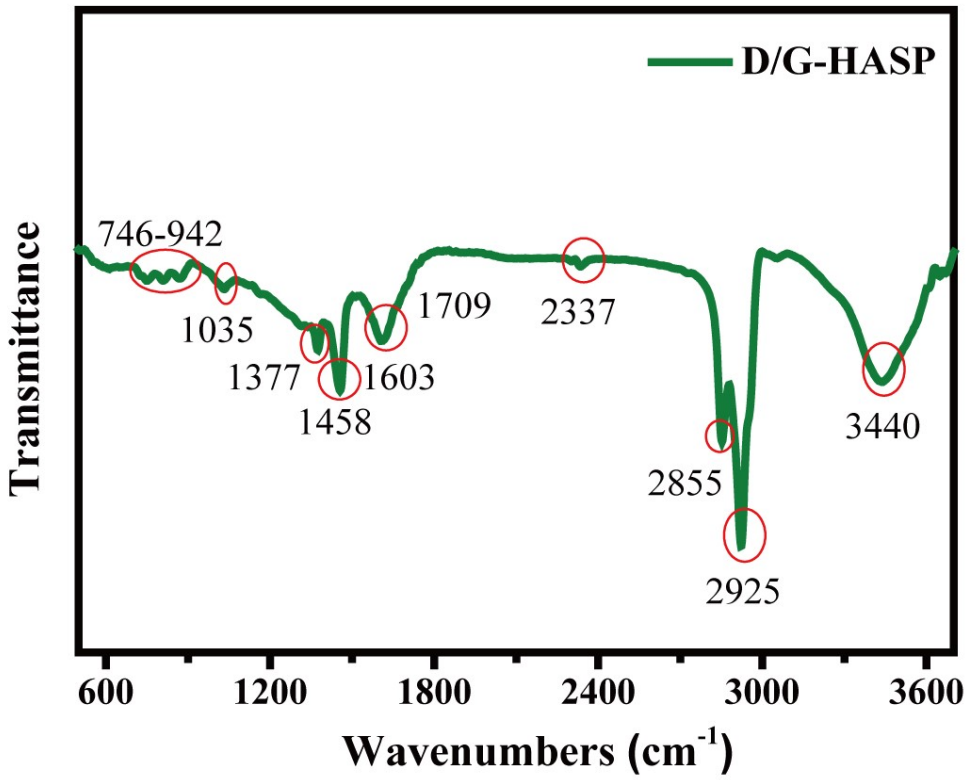

Fig. S5 FTIR spectra of D/G-HASP catalyst.

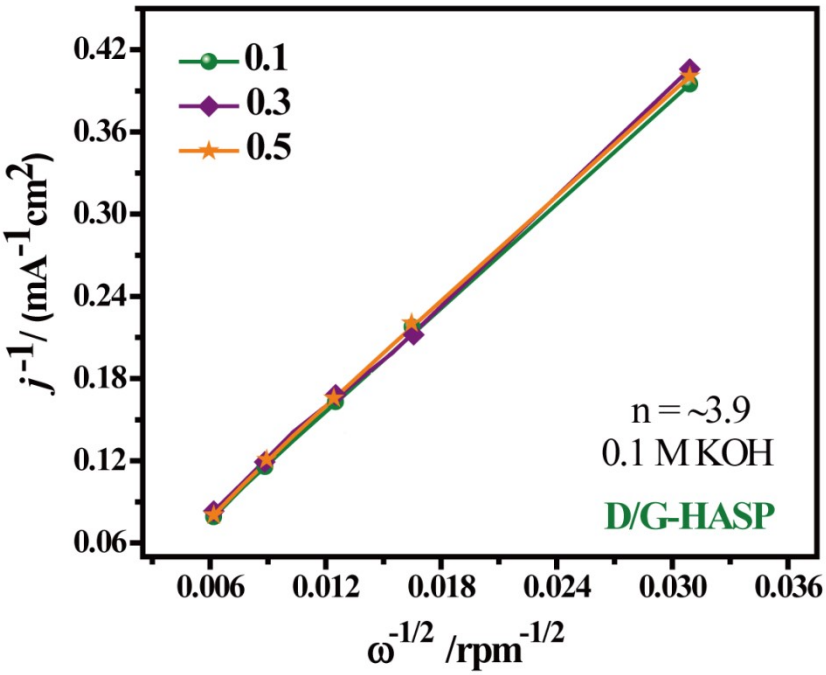

Fig. S6 Koutecky-Levich plot for electron transfer number (n) of the D/G-HASP catalyst.

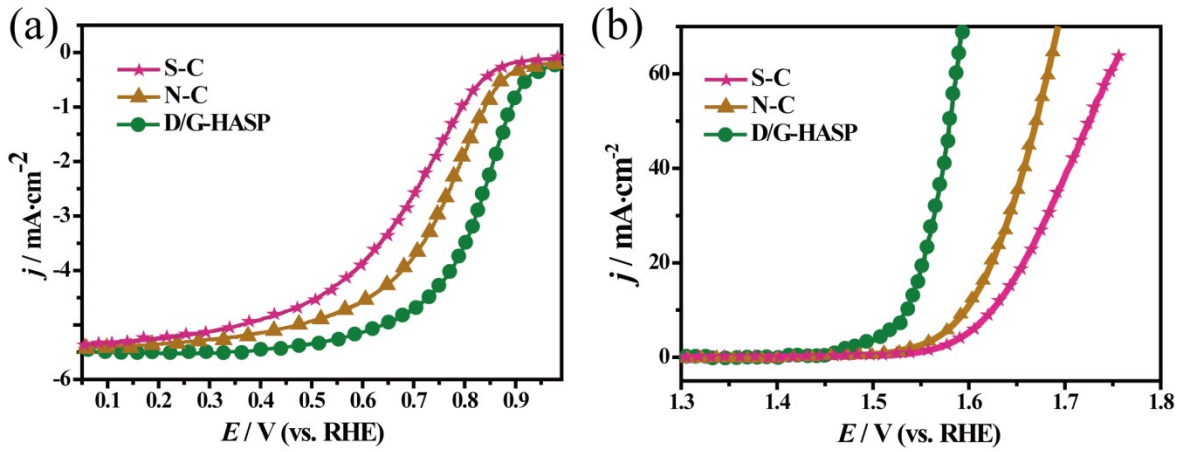

Fig. S7 (a) ORR polarization curve (b) OER polarization curve.

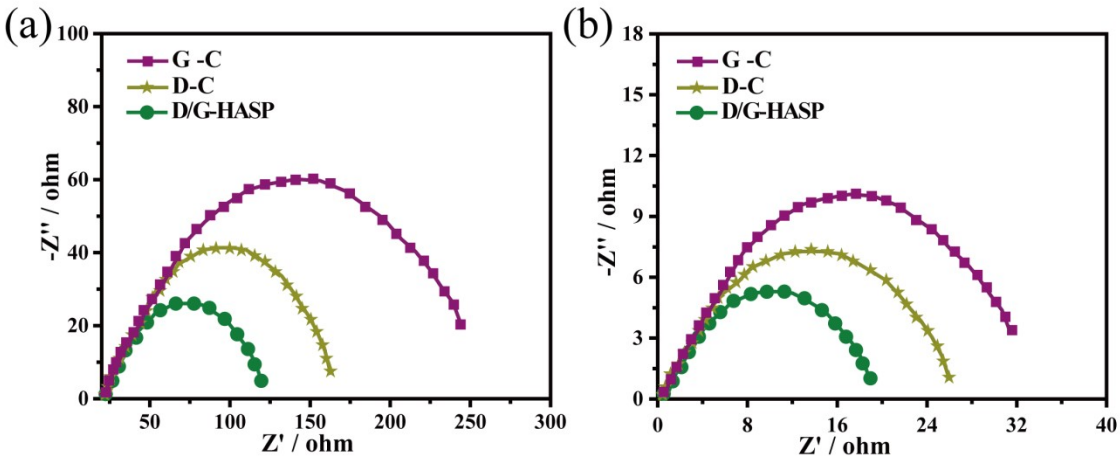

Fig. S8 (a) Nyquist plots for the ORR (b) Nyquist plots for the OER.

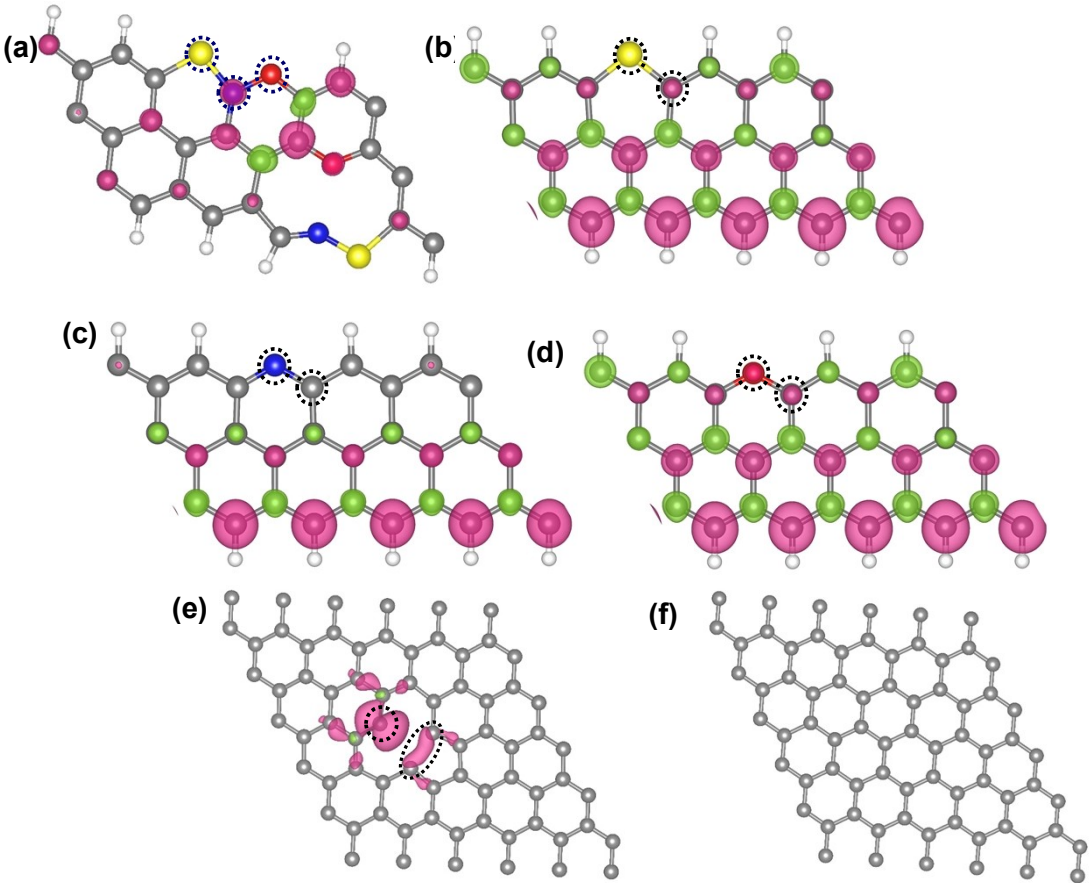

Fig. S9 The spin density of (a) S, N, O co-doped asphaltene, (b) mono S-doped asphaltene, (c) mono N-doped asphaltene, (d) mono O-doped asphaltene, (e) mono vacancy graphene and (f) pristine graphene. The iso-surface of 0.002 e $Å^{-3}$. The red and green color represents spin-up and spin-down respectively. The black circle surrounding atoms represents active sites for ORR intermediates adsorption

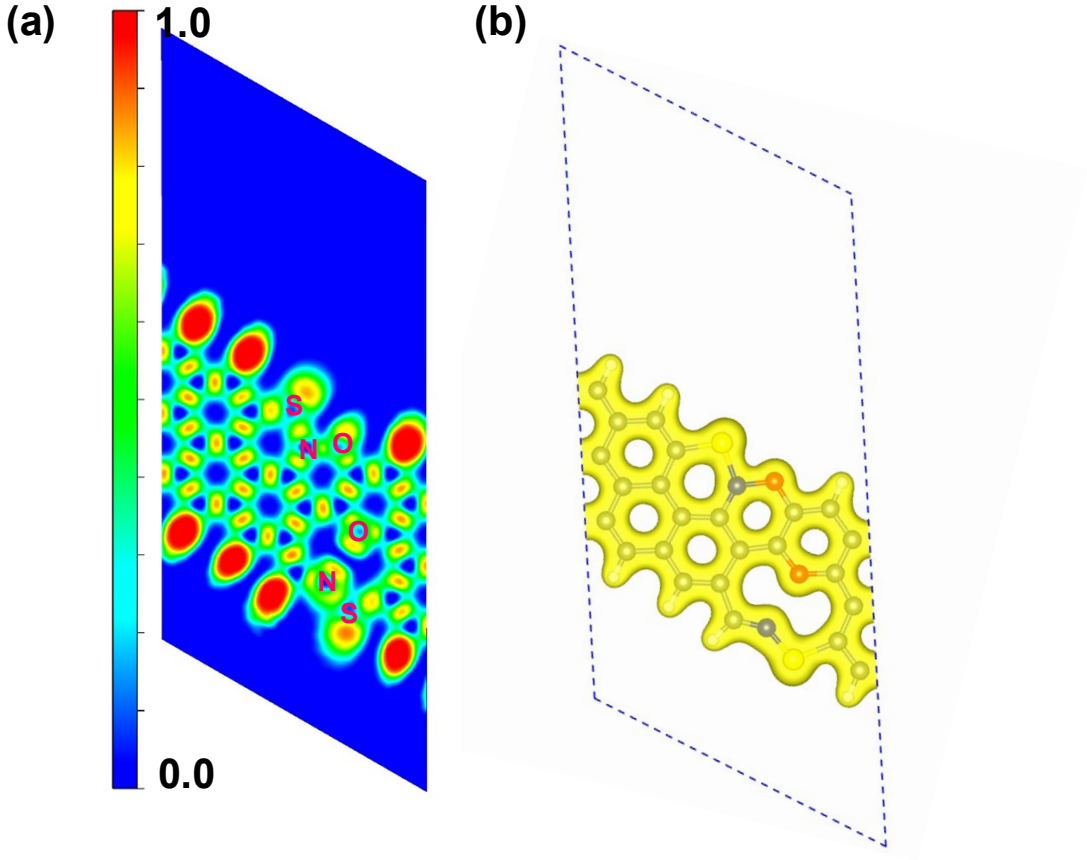

Fig. S10 (a) Electron location function and (b) charge density distribution of D/G-HASP. The iso-surface of 0.07 e $Å^{-3}$.

Table S1. Elemental analysis of the D/G-HASP by EDS and XPS.

Elements	Elemental analysis EDS (wt%)	XPS analysis (atom%)
C	76.32	87.375
N	12.65	4.648
S	6.72	3.129
O	4.31	4.848

Table S2. The DFT energies (E_{DFT}), zero-point energies (E_{ZPE}), and entropies (TS) for the gas molecules involved in ORR. All values are given in eV. The gas-phase H_2O at 0.035 bar is taken as a reference since it is in equilibrium with liquid H_2O at this pressure. The vibrational corrections are taken from ref.[10]

Species	E_{DFT}	E_{ZPE}	TS	G
H_2	-6.77	0.27	0.40	-6.9
H_2O	-14.69	0.57	0.67 (0.035 bar)	-14.79
O_2	-10.13	0.10	0.63	-10.66

Table S3. DFT total energies (E_{DFT}), zero-point energies (E_{ZPE}), entropies multiplied by T (= 298.15 K) (TS), free energies (G), and relative free energies (ΔG) of ORR intermediates in an alkaline medium for N-site in D/G-HASP. All values are calculated in eV.

N-site	E_{DFT}	E_{ZPE}	TS	G	ΔG	ΔG_n
U=0.00 V						
Step(1) *	-275.803	0.00	0.00	-275.803	4.920	ΔG_1 (-1.027)
Step(2)(OOH)*	-291.369	0.450	0.221	-291.140	3.893	ΔG_2 (-1.558)
Step(3) O*	-281.441	0.095	0.042	-281.388	2.305	ΔG_3 (-1.03)
Step(4) OH*	-286.189	0.388	0.071	-285.872	1.271	ΔG_4 (-1.271)
U=0.20 V						
Step(1) *	-275.803	0.00	0.00	-275.803	4.12	ΔG_1 (-0.827)
Step(2)(OOH)*	-291.369	0.450	0.221	-291.140	3.293	ΔG_2 (-1.388)
Step(3) O*	-281.441	0.095	0.042	-281.388	1.905	ΔG_3 (-0.834)
Step(4) OH*	-286.189	0.388	0.071	-285.872	1.071	ΔG_4 (-1.071)
U=0.40 V						
Step(1) *	-275.803	0.00	0.00	-275.803	3.32	ΔG_1 (-0.627)
Step(2)(OOH)*	-291.369	0.450	0.221	-291.140	2.693	ΔG_2 (-1.188)
Step(3) O*	-281.441	0.095	0.042	-281.388	1.505	ΔG_3 (-0.634)
Step(4) OH*	-286.189	0.388	0.071	-285.872	0.871	ΔG_4 (-0.871)
U=0.80 V						
Step(1) *	-275.803	0.00	0.00	-275.803	1.72	ΔG_1 (-0.227)
Step(2)(OOH)*	-291.369	0.450	0.221	-291.140	1.493	ΔG_2 (-0.788)
Step(3) O*	-281.441	0.095	0.042	-281.388	0.705	ΔG_3 (-0.234)
Step(4) OH*	-286.189	0.388	0.071	-285.872	0.471	ΔG_4 (-0.471)
U=1.23 V						
Step(1) *	-275.803	0.00	0.00	-275.803	0	ΔG_1 (0.203)
Step(2)(OOH)*	-291.369	0.450	0.221	-291.140	0.203	ΔG_2 (-0.358)
Step(3) O*	-281.441	0.095	0.042	-281.388	-0.155	ΔG_3 (0.196)
Step(4) OH*	-286.189	0.388	0.071	-285.872	0.041	ΔG_4 (-0.041)

Table S4. DFT total energies (E_{DFT}), zero-point energies (E_{ZPE}), entropies multiplied by T (= 298.15 K) (TS), free energies (G), and relative free energies (ΔG) of ORR intermediates in an alkaline medium for S-site in D/G-HASP. All values are calculated in eV.

S-site	E_{DFT}	E_{ZPE}	TS	G	ΔG	ΔG_n
U=0.00 V						
Step(1) *	-275.803	0.00	0.00	-275.803	4.920	ΔG_1 (-0.554)
Step(2)(OOH)*	-290.913	0.443	0.197	-290.667	4.366	ΔG_2 (-1.816)
Step(3) O*	-281.196	0.083	0.030	-281.143	2.550	ΔG_3 (-1.172)
Step(4) OH*	-286.045	0.369	0.089	-285.765	1.378	ΔG_4 (-1.378)
U=0.20 V						
Step(1) *	-275.803	0.00	0.00	-275.803	4.12	ΔG_1 (-0.354)
Step(2)(OOH)*	-290.913	0.443	0.197	-290.667	3.766	ΔG_2 (-1.616)
Step(3) O*	-281.196	0.083	0.030	-281.143	2.150	ΔG_3 (-0.972)
Step(4) OH*	-286.045	0.369	0.089	-285.765	1.178	ΔG_4 (-1.178)
U=0.40 V						
Step(1) *	-275.803	0.00	0.00	-275.803	3.32	ΔG_1 (-0.154)
Step(2)(OOH)*	-290.913	0.443	0.197	-290.667	3.166	ΔG_2 (-1.416)
Step(3) O*	-281.196	0.083	0.030	-281.143	1.750	ΔG_3 (-0.772)
Step(4) OH*	-286.045	0.369	0.089	-285.765	0.978	ΔG_4 (-0.978)
U=0.80 V						
Step(1) *	-275.803	0.00	0.00	-275.803	1.72	ΔG_1 (0.246)
Step(2)(OOH)*	-290.913	0.443	0.197	-290.667	1.966	ΔG_2 (-1.016)
Step(3) O*	-281.196	0.083	0.030	-281.143	0.950	ΔG_3 (-0.372)
Step(4) OH*	-286.045	0.369	0.089	-285.765	0.578	ΔG_4 (-0.578)
U=1.23 V						
Step(1) *	-275.803	0.00	0.00	-275.803	0	ΔG_1 (0.676)
Step(2)(OOH)*	-290.913	0.443	0.197	-290.667	0.676	ΔG_2 (-0.586)
Step(3) O*	-281.196	0.083	0.030	-281.143	0.090	ΔG_3 (0.058)
Step(4) OH*	-286.045	0.369	0.089	-285.765	0.148	ΔG_4 (-0.148)

Table S5. DFT total energies (E_{DFT}), zero-point energies (E_{ZPE}), entropies multiplied by T (= 298.15 K) (TS), free energies (G), and relative free energies (ΔG) of ORR intermediates in an alkaline medium for O-site in D/G-HASP. All values are calculated in eV.

O-site	E_{DFT}	E_{ZPE}	TS	G	ΔG	ΔG_n
U=0.00 V						
Step(1) *	-275.803	0.00	0.00	-275.803	4.920	ΔG_1 (-0.508)
Step(2)(OOH)*	-290.947	0.470	0.144	-290.621	4.412	ΔG_2 (-1.749)
Step(3) O*	-281.020	0.062	0.072	-281.030	2.663	ΔG_3 (-1.421)
Step(4) OH*	-286.104	0.326	0.123	-285.901	1.242	ΔG_4 (-1.242)
U=0.20 V						
Step(1) *	-275.803	0.00	0.00	-275.803	4.12	ΔG_1 (-0.308)
Step(2)(OOH)*	-290.947	0.470	0.144	-290.621	3.812	ΔG_2 (-1.549)
Step(3) O*	-281.020	0.062	0.072	-281.030	2.263	ΔG_3 (-1.221)
Step(4) OH*	-286.104	0.326	0.123	-285.901	1.042	ΔG_4 (-1.042)
U=0.40 V						
Step(1) *	-275.803	0.00	0.00	-275.803	3.32	ΔG_1 (-0.108)
Step(2)(OOH)*	-290.947	0.470	0.144	-290.621	3.212	ΔG_2 (-1.349)
Step(3) O*	-281.020	0.062	0.072	-281.030	1.863	ΔG_3 (-1.021)
Step(4) OH*	-286.104	0.326	0.123	-285.901	0.842	ΔG_4 (-0.842)
U=0.80 V						
Step(1) *	-275.803	0.00	0.00	-275.803	1.72	ΔG_1 (0.292)
Step(2)(OOH)*	-290.947	0.470	0.144	-290.621	2.012	ΔG_2 (-0.949)
Step(3) O*	-281.020	0.062	0.072	-281.030	1.063	ΔG_3 (-0.621)
Step(4) OH*	-286.104	0.326	0.123	-285.901	0.442	ΔG_4 (-0.442)
U=1.23 V						
Step(1) *	-275.803	0.00	0.00	-275.803	0	ΔG_1 (0.722)
Step(2)(OOH)*	-290.947	0.470	0.144	-290.621	0.722	ΔG_2 (-0.519)
Step(3) O*	-281.020	0.062	0.072	-281.030	0.203	ΔG_3 (-0.191)
Step(4) OH*	-286.104	0.326	0.123	-285.901	0.012	ΔG_4 (-0.012)

Table S6. DFT total energies (E_{DFT}), zero-point energies (E_{ZPE}), entropies multiplied by T (= 298.15 K) (TS), free energies (G), and relative free energies (ΔG) of ORR intermediates in an alkaline medium for C-site in N doped asphaltene. All values are calculated in eV.

C-site	E_{DFT}	E_{ZPE}	TS	G	ΔG	ΔG_n
U=0.00 V						
Step(1) *	-305.072	0.00	0.00	-305.072	4.920	ΔG_1 (0.283)
Step(2)(OOH)*	-319.430	0.474	0.143	-319.099	5.203	ΔG_2 (-2.22)
Step(3) O*	-310.062	0.791	0.710	-309.981	2.981	ΔG_3 (-1.168)
Step(4) OH*	-314.912	0.363	0.050	-314.599	1.813	ΔG_4 (-1.813)
U=0.20 V						
Step(1) *	-305.072	0.00	0.00	-305.072	4.12	ΔG_1 (0.483)
Step(2)(OOH)*	-319.430	0.474	0.143	-319.099	4.603	ΔG_2 (-2.022)
Step(3) O*	-310.062	0.791	0.710	-309.981	2.581	ΔG_3 (-0.968)
Step(4) OH*	-314.912	0.363	0.050	-314.599	1.613	ΔG_4 (-1.613)
U=0.40 V						
Step(1) *	-305.072	0.00	0.00	-305.072	3.32	ΔG_1 (0.683)
Step(2)(OOH)*	-319.430	0.474	0.143	-319.099	4.003	ΔG_2 (-1.822)
Step(3) O*	-310.062	0.791	0.710	-309.981	2.181	ΔG_3 (-0.768)
Step(4) OH*	-314.912	0.363	0.050	-314.599	1.413	ΔG_4 (-1.413)
U=0.80 V						
Step(1) *	-305.072	0.00	0.00	-305.072	1.72	ΔG_1 (1.083)
Step(2)(OOH)*	-319.430	0.474	0.143	-319.099	2.803	ΔG_2 (-1.422)
Step(3) O*	-310.062	0.791	0.710	-309.981	1.381	ΔG_3 (-0.368)
Step(4) OH*	-314.912	0.363	0.050	-314.599	1.013	ΔG_4 (-1.013)
U=1.23 V						
Step(1) *	-305.072	0.00	0.00	-305.072	0	ΔG_1 (1.513)
Step(2)(OOH)*	-319.430	0.474	0.143	-319.099	1.513	ΔG_2 (-0.992)
Step(3) O*	-310.062	0.791	0.710	-309.981	0.521	ΔG_3 (0.062)
Step(4) OH*	-314.912	0.363	0.050	-314.599	0.583	ΔG_4 (-0.583)

Table S7. DFT total energies (E_{DFT}), zero-point energies (E_{ZPE}), entropies multiplied by T (= 298.15 K) (TS), free energies (G), and relative free energies (ΔG) of ORR intermediates in an alkaline medium for C-site in S doped asphaltene. All values are calculated in eV.

C-site	E_{DFT}	E_{ZPE}	TS	G	ΔG	ΔG_n
U=0.00 V						
Step(1) *	-300.885	0.00	0.00	-300.885	4.920	ΔG_1 (0.032)
Step(2)(OOH)*	-315.479	0.461	0.145	-315.163	4.952	ΔG_2 (-2.498)
Step(3) O*	-306.392	0.098	0.027	-306.321	2.454	ΔG_3 (-0.886)
Step(4) OH*	-310.968	0.384	0.073	-310.657	1.568	ΔG_4 (-1.586)
U=0.20 V						
Step(1) *	-300.885	0.00	0.00	-300.885	4.12	ΔG_1 (0.232)
Step(2)(OOH)*	-315.479	0.461	0.145	-315.163	4.352	ΔG_2 (-2.298)
Step(3) O*	-306.392	0.098	0.027	-306.321	2.054	ΔG_3 (-0.686)
Step(4) OH*	-310.968	0.384	0.073	-310.657	1.368	ΔG_4 (-1.368)
U=0.40 V						
Step(1) *	-300.885	0.00	0.00	-300.885	3.32	ΔG_1 (0.432)
Step(2)(OOH)*	-315.479	0.461	0.145	-315.163	3.752	ΔG_2 (-2.098)
Step(3) O*	-306.392	0.098	0.027	-306.321	1.654	ΔG_3 (-0.486)
Step(4) OH*	-310.968	0.384	0.073	-310.657	1.168	ΔG_4 (-1.168)
U=0.80 V						
Step(1) *	-300.885	0.00	0.00	-300.885	1.72	ΔG_1 (0.832)
Step(2)(OOH)*	-315.479	0.461	0.145	-315.163	2.552	ΔG_2 (-1.698)
Step(3) O*	-306.392	0.098	0.027	-306.321	0.854	ΔG_3 (-0.086)
Step(4) OH*	-310.968	0.384	0.073	-310.657	0.768	ΔG_4 (-0.768)
U=1.23 V						
Step(1) *	-300.885	0.00	0.00	-300.885	0	ΔG_1 (1.262)
Step(2)(OOH)*	-315.479	0.461	0.145	-315.163	1.262	ΔG_2 (-1.268)
Step(3) O*	-306.392	0.098	0.027	-306.321	-0.006	ΔG_3 (0.344)
Step(4) OH*	-310.968	0.384	0.073	-310.657	0.338	ΔG_4 (-0.338)

Table S8. DFT total energies (E_{DFT}), zero-point energies (E_{ZPE}), entropies multiplied by T (= 298.15 K) (TS), free energies (G), and relative free energies (ΔG) of ORR intermediates in an alkaline medium for C-site in O-doped asphaltene. All values are calculated in eV.

C-site	E_{DFT}	E_{ZPE}	TS	G	ΔG	ΔG_n
U=0.00 V						
Step(1) *	-303.660	0.00	0.00	-303.660	4.920	ΔG_1 (0.168)
Step(2)(OOH)*	-318.124	0.466	0.144	-317.802	5.088	ΔG_2 (-2.647)
Step(3) O*	-309.184	0.100	0.025	-309.109	2.441	ΔG_3 (-0.810)
Step(4) OH*	-313.697	0.392	0.064	-313.369	1.631	ΔG_4 (-1.631)
U=0.20 V						
Step(1) *	-303.660	0.00	0.00	-303.660	4.12	ΔG_1 (-0.368)
Step(2)(OOH)*	-318.124	0.466	0.144	-317.802	4.488	ΔG_2 (-2.447)
Step(3) O*	-309.184	0.100	0.025	-309.109	2.041	ΔG_3 (-0.410)
Step(4) OH*	-313.697	0.392	0.064	-313.369	1.431	ΔG_4 (-1.431)
U=0.40 V						
Step(1) *	-303.660	0.00	0.00	-303.660	3.32	ΔG_1 (0.568)
Step(2)(OOH)*	-318.124	0.466	0.144	-317.802	3.888	ΔG_2 (-2.247)
Step(3) O*	-309.184	0.100	0.025	-309.109	1.641	ΔG_3 (-0.410)
Step(4) OH*	-313.697	0.392	0.064	-313.369	1.231	ΔG_4 (-1.231)
U=0.80 V						
Step(1) *	-303.660	0.00	0.00	-303.660	1.72	ΔG_1 (0.968)
Step(2)(OOH)*	-318.124	0.466	0.144	-317.802	2.688	ΔG_2 (-1.847)
Step(3) O*	-309.184	0.100	0.025	-309.109	0.841	ΔG_3 (-0.010)
Step(4) OH*	-313.697	0.392	0.064	-313.369	0.831	ΔG_4 (-0.831)
U=1.23 V						
Step(1) *	-303.660	0.00	0.00	-303.660	0	ΔG_1 (1.398)
Step(2)(OOH)*	-318.124	0.466	0.144	-317.802	1.398	ΔG_2 (-1.417)
Step(3) O*	-309.184	0.100	0.025	-309.109	-0.019	ΔG_3 (0.420)
Step(4) OH*	-313.697	0.392	0.064	-313.369	0.401	ΔG_4 (-0.401)

Table S9. DFT total energies (E_{DFT}), zero-point energies (E_{ZPE}), entropies multiplied by T (= 298.15 K) (TS), free energies (G), and relative free energies (ΔG) of ORR intermediates in an alkaline medium for mono vacancy defective graphene. All values are calculated in eV.

C-site	E_{DFT}	E_{ZPE}	TS	G	ΔG	ΔG_n
U=0.00 V						
Step(1) *	-650.134	0.00	0.00	-650.134	4.920	ΔG_1 (-1.220)
Step(2)(OOH)*	-665.952	0.452	0.164	-665.664	3.700	ΔG_2 (-3.914)
Step(3) O*	-658.310	0.108	0.036	-658.238	-0.214	ΔG_3 (-1.172)
Step(4) OH*	-660.899	0.416	0.033	-660.516	0.958	ΔG_4 (-0.958)
U=0.20 V						
Step(1) *	-650.134	0.00	0.00	-650.134	4.12	ΔG_1 (-1.020)
Step(2)(OOH)*	-665.952	0.452	0.164	-665.664	3.100	ΔG_2 (-3.714)
Step(3) O*	-658.310	0.108	0.036	-658.238	-0.614	ΔG_3 (1.372)
Step(4) OH*	-660.899	0.416	0.033	-660.516	0.758	ΔG_4 (-0.758)
U=0.40 V						
Step(1) *	-650.134	0.00	0.00	-650.134	3.32	ΔG_1 (-0.820)
Step(2)(OOH)*	-665.952	0.452	0.164	-665.664	2.500	ΔG_2 (-3.514)
Step(3) O*	-658.310	0.108	0.036	-658.238	-1.014	ΔG_3 (1.572)
Step(4) OH*	-660.899	0.416	0.033	-660.516	0.558	ΔG_4 (-0.558)
U=0.80 V						
Step(1) *	-650.134	0.00	0.00	-650.134	1.72	ΔG_1 (-0.420)
Step(2)(OOH)*	-665.952	0.452	0.164	-665.664	1.300	ΔG_2 (-3.114)
Step(3) O*	-658.310	0.108	0.036	-658.238	-1.814	ΔG_3 (1.972)
Step(4) OH*	-660.899	0.416	0.033	-660.516	0.158	ΔG_4 (-0.158)
U=1.23 V						
Step(1) *	-650.134	0.00	0.00	-650.134	0	ΔG_1 (0.010)
Step(2)(OOH)*	-665.952	0.452	0.164	-665.664	0.010	ΔG_2 (-2.684)
Step(3) O*	-658.310	0.108	0.036	-658.238	-2.674	ΔG_3 (2.402)
Step(4) OH*	-660.899	0.416	0.033	-660.516	-0.272	ΔG_4 (0.272)

Table S10. DFT total energies (E_{DFT}), zero-point energies (E_{ZPE}), entropies multiplied by T (= 298.15 K) (TS), free energies (G), and relative free energies (ΔG) of ORR intermediates in an alkaline medium for pristine graphene. All values are calculated in eV.

C-site	E_{DFT}	E_{ZPE}	TS	G	ΔG	ΔG_n
U=0.00 V						
Step(1) *	-666.975	0.00	0.00	-666.975	4.920	ΔG_1 (1.376)
Step(2)(OOH)*	-680.090	0.381	0.200	-679.909	6.296	ΔG_2 (-2.372)
Step(3) O*	-671.015	0.099	0.025	-670.941	3.924	ΔG_3 (-0.914)
Step(4) OH*	-675.608	0.378	0.075	-675.305	3.010	ΔG_4 (-3.010)
U=0.20 V						
Step(1) *	-666.975	0.00	0.00	-666.975	4.12	ΔG_1 (1.576)
Step(2)(OOH)*	-680.090	0.381	0.200	-679.909	5.696	ΔG_2 (-2.172)
Step(3) O*	-671.015	0.099	0.025	-670.941	3.524	ΔG_3 (-0.714)
Step(4) OH*	-675.608	0.378	0.075	-675.305	2.810	ΔG_4 (-2.810)
U=0.40 V						
Step(1) *	-666.975	0.00	0.00	-666.975	3.32	ΔG_1 (1.776)
Step(2)(OOH)*	-680.090	0.381	0.200	-679.909	5.096	ΔG_2 (-1.972)
Step(3) O*	-671.015	0.099	0.025	-670.941	3.124	ΔG_3 (-0.514)
Step(4) OH*	-675.608	0.378	0.075	-675.305	2.610	ΔG_4 (-2.610)
U=0.80 V						
Step(1) *	-666.975	0.00	0.00	-666.975	1.72	ΔG_1 (2.176)
Step(2)(OOH)*	-680.090	0.381	0.200	-679.909	3.896	ΔG_2 (-1.572)
Step(3) O*	-671.015	0.099	0.025	-670.941	2.324	ΔG_3 (-0.114)
Step(4) OH*	-675.608	0.378	0.075	-675.305	2.210	ΔG_4 (-2.210)
U=1.23 V						
Step(1) *	-666.975	0.00	0.00	-666.975	0	ΔG_1 (2.606)
Step(2)(OOH)*	-680.090	0.381	0.200	-679.909	2.606	ΔG_2 (-1.142)
Step(3) O*	-671.015	0.099	0.025	-670.941	1.464	ΔG_3 (0.316)
Step(4) OH*	-675.608	0.378	0.075	-675.305	1.780	ΔG_4 (-1.780)

Table S11. The charge (Q |e|) and spin difference (SD) analysis of S, N, O co-doped asphaltene (D/G-HASP) mono S-doped asphaltene (S-asphaltene), mono N-doped asphaltene (N-asphaltene), mono O-doped asphaltene (O-asphaltene), mono-vacancy graphene and pristine graphene respectively.

System	Q|e|	SD
D/G-HASP	+3.82	+0.99
S-asphaltene	+4.02	+0.91
N-asphaltene	+3.98	+0.82
O-asphaltene	+4.01	+0.92
m-VacG	+9.04	+1.07
Pristine-G	$+1x10^{-4}$	$-1x10^{-4}$

Table S12. Comparison of the ORR/OER performance of D/G-HASP catalyst with literature reprints electrocatalysts in alkaline electrolytes.

Electrocatalysts	E_{ORR} ($E_{1/2}$ V vs. RHE) (V)	E_{OER} at E_j =10 mA cm^{-2} (V)	Oxygen Activity ΔE (Ej_{10}-$E_{1/2}$) (V)	Reference
D/G-HASP	**0.840**	**1.54**	**0.7**	**This work**
NBCCFe/N-rGO	0.848	1.609	0.761	11
Fe-NiNC-50	0.850	1.57	0.72	12
C-MOF-C2-900	0.815	1.651	0.836	13
g-CN-CNF-50wt	0.814	1.652	0.838	14
NiFeP@3D-FeNC	0.840	1.48	0.64	15
ZIF-67@NPC-2(2:1)	0.820	1.64	0.82	16
CNCN-44	0.800	1.61	0.81	17
Co_3O_4/NPGC	0.850	1.68	0.83	18
CoXNi-N/C	0.840	1.59	0.75	19
Co-NCNT	0.860	1.63	0.77	20
S-Co9-xFexS8@rGO-10	0.840	1.52	0.68	21
NKCNPs-900	0.790	1.71	0.92	22

Table S13. Comparison of rechargeable zinc-air battery performance of D/G-HASP catalyst with other reported air electrocatalysts of zinc-air batteries.

Air catalysts	Open circuit voltage (V)	Cycling Stability (No. of Cycles)	Cycling Stability Time (h)	Current density (@mA.cm^{-2})	Reference
D/G-HASP	**1.50**	**500**	**50**	**10**	**This work**
CoNi/BCF	1.44	180	30	10	[23]
Fe-NiNC-50	1.41	600	100	5	[12]
porous PVA-1 wt.% SiO_2	1.42	144	48	3	[24]
C-MOF-C2-900	1.46	360	120	2	[25]
Co-N-CNTs	1.36	130	15	2	[26]
NCNT/CoO-NiO-NiCo	~	100	17	20	[27]
Co-NCNT	1.45	400	72	2	[20]
$NiCo_2S_4$/CB	1.57	550	~	10	[28]
Fe_3Pt/Ni_3FeN	~	240	500	10	[29]

References

1. S. Chiaberge, G. Guglielmetti, L. Montanari, M. Salvalaggio, L. Santolini, S. Spera and P. Cesti, *Energy Fuels*, 2009, **23**, 4486-4495.
2. H. Wu and M. R. Kessler, *RSC Adv.*, 2015, **5**, 24264-24273.
3. G. Yasin, M. A. Khan, M. Arif, M. Shakeel, T. M. Hassan, W. Q. Khan, R. M. Korai, Z. Abbas and Y. Zuo, *J. Alloys Compd.*, 2018, **755**, 79-88.
4. B. Hammer, L. B. Hansen and J. K. Nørskov, *Phys. Rev. B*, 1999, **59**, 7413-7421.
5. G. Kresse and J. Furthmüller, *Comput. Mater. Sci.,* 1996, **6**, 15-50.
6. G. Kresse and J. Furthmüller, *Phys. Rev. B*, 1996, **54**, 11169-11186.
7. G. Kresse and J. Hafner, *Phys. Rev. B*, 1993, **47**, 558-561.
8. S. Grimme, J. Antony, S. Ehrlich and H. Krieg, *The J. Chem. Phys.,* 2010, **132**, 154104.
9. J. K. Nørskov, J. Rossmeisl, A. Logadottir, L. Lindqvist, J. R. Kitchin, T. Bligaard and H. Jónsson, *The J. Chem. Phys. B*, 2004, **108**, 17886-17892.
10. A. A. Peterson, F. Abild-Pedersen, F. Studt, J. Rossmeisl and J. K. Nørskov, *Energy Environ. Sci.*, 2010, **3**, 1311-1315.
11. N.-I. Kim, S.-H. Cho, S. H. Park, Y. J. Lee, R. A. Afzal, J. Yoo, Y.-S. Seo, Y. J. Lee and J.-Y. Park, *J. Mater. Chem. A*, 2018, **6**, 17807-17818.
12. X. Zhu, D. Zhang, C.-J. Chen, Q. Zhang, R.-S. Liu, Z. Xia, L. Dai, R. Amal and X. Lu, *Nano Energy*, 2020, **71**, 104597.
13. M. Zhang, Q. Dai, H. Zheng, M. Chen and L. Dai, *Adv. Mater.*, 2018, **30**.
14. J. E. Park, M.-J. Kim, M. S. Lim, S. Y. Kang, J. K. Kim, S.-H. Oh, M. Her, Y.-H. Cho and Y.-E. Sung, *Appl. Catal. B-Environ.*, 2018, **237**, 140-148.
15. S. Ibraheem, S. Chen, J. Li, W. Li, X. Gao, Q. Wang and Z. Wei, *ACS Appl. Mater. Interfaces*, 2019, 11, 699-705.
16. H. Wang, F.-X. Yin, B.-H. Chen, X.-B. He, P.-L. Lv, C.-Y. Ye and D.-J. Liu, *Appl. Catal. B-Environ.*, 2017, **205**, 55-67.

17. J. Song, C. Zhu, S. Fu, Y. Song, D. Du and Y. Lin, *J. Mater. Chem. A*, 2016, **4**, 4864-4870.

18. G. Li, X. Wang, J. Fu, J. Li, M. G. Park, Y. Zhang, G. Lui and Z. Chen, *Angew. Chem. Int. Ed.*, 2016, **55**, 4977-4982.

19. Z. Li, H. He, H. Cao, S. Sun, W. Diao, D. Gao, P. Lu, S. Zhang, Z. Guo, M. Li, R. Liu, D. Ren, C. Liu, Y. Zhang, Z. Yang, J. Jiang and G. Zhang, *Appl. Catal. B-Environ.*, 2019, **240**, 112-121.

20. Z. Pei, Y. Huang, Z. Tang, L. Ma, Z. Liu, Q. Xue, Z. Wang, H. Li, Y. Chen and C. Zhi, *Energy Storage Mater.*, 2019, **20**, 234-242.

21. M. Zeng, Y. Liu, F. Zhao, K. Nie, N. Han, X. Wang, W. Huang, X. Song, J. Zhong and Y. Li, *Adv. Funct. Mater.*, 2016, **26**, 4397-4404.

22. Q. Wang, Y. Lei, Y. Zhu, H. Wang, J. Feng, G. Ma, Y. Wang, Y. Li, B. Nan, Q. Feng, Z. Lu and H. Yu, *ACS Appl. Mater.*, 2018, **10**, 29448-29456.

23. W. Wan, X. Liu, H. Li, X. Peng, D. Xi and J. Luo, *Appl. Catal. B-Environ.*, 2019, **240**, 193-200.

24. X. Fan, J. Liu, Z. Song, X. Han, Y. Deng, C. Zhong and W. Hu, *Nano Energy*, 2019, **56**, 454-462.

25. M. Zhang, Q. Dai, H. Zheng, M. Chen and L. Dai, *Adv. Mater.*, 2018, **30**, 1705431.

26. T. Wang, Z. Kou, S. Mu, J. Liu, D. He, I. S. Amiinu, W. Meng, K. Zhou, Z. Luo, S. Chaemchuen and F. Verpoort, *Adv. Funct. Mater.*, 2018, **28**, 1705048.

27. X. Liu, M. Park, M. G. Kim, S. Gupta, G. Wu and J. Cho, *Angew. Chem. Int. Ed.*, 2015, **54**, 9654-9658.

28. N. Tangaemsakul, A. Kannan and N. Tantavichet, *J. Alloys Compd.*, 2021, **873**, 159749.

29. Z. Cui, G. Fu, Y. Li and J. B. Goodenough, *Angew. Chem. Int. Ed.*, 2017, **56**, 9901-9905.